The Plant Journal (1999) **19**(5), 555–567

Characterization of the unconventional myosin VIII in plant cells and its localization at the post-cytokinetic cell wall

Stefanie Reichelt[1,2,†], Alex E. Knight[1,‡], Tony P. Hodge[1], Frantisek Baluska[2,3], Jozef Samaj[2,4], Dieter Volkmann[2] and John Kendrick-Jones[1,*]

[1]*Structural Studies Division, MRC Laboratory of Molecular Biology, Hills Road, Cambridge CB2 2QH, UK,*
[2]*Botanisches Institut, Universität Bonn, Venusbergweg 22, D-53115 Bonn, Germany,*
[3]*Institute of Botany, Slovak Academy of Sciences, Dúbravská cesta 14, SK-84223 Bratislava, Slovakia, and*
[4]*Institute of Plant Genetics, Slovak Academy of Sciences, Akademicka 2, SK-95007, Slovakia*

Summary

Myosins are a large superfamily of motor proteins which, in association with actin, are involved in intracellular motile processes. In addition to the conventional myosins involved in muscle contractility, there is, in animal cells, a wide range of unconventional myosins implicated in membrane-associated processes, such as vesicle transport and membrane dynamics. In plant cells, however, very little is known about myosins. We have raised an antibody to the recombinant tail region of *Arabidopsis thaliana* myosin 1 (a class VIII myosin) and used it in immunofluorescence and EM studies on root cells from cress and maize. The plant myosin VIII is found to be concentrated at newly formed cross walls at the stage in which the phragmoplast cytoskeleton has depolymerized and the new cell plate is beginning to mature. These walls are rich in plasmodesmata and we show that they are the regions where the longitudinal actin cables appear to attach. Myosin VIII appears to be localized in these plasmodesmata and we suggest that this protein is involved in maturation of the cell plate and the re-establishment of cytoplasmic actin cables at sites of intercellular communication.

Introduction

The myosins are a large superfamily of molecular motors which generate movement and mechanical force in ATP-dependent interactions with actin filaments. On the basis of their conserved head or motor domain sequences, i.e. the highly conserved region containing the ATPase and actin binding sites, the myosins can be divided into at least 14 classes (designated I to XIV) (Cope *et al.*, 1996; Mermall *et al.*, 1998). In addition, each class of myosin contains tail domains which are characteristic for each myosin and are believed to be responsible for the specific subcellular localization and function of these motors.

In unicellular systems and mammalian cells the involvement of the conventional two-headed, filament-forming myosins (myosin IIs) is well established in muscular contraction and cytoplasmic contractile events such as cytokinesis. In addition, the so-called unconventional myosins of class I, V and VI are now relatively well described; several of them have recently been shown to be involved in various actin-based and membrane-associated functions, which include vesicle transport, cytokinesis and such specialized functions as auditory perception (for recent reviews see Bähler, 1996; Fath and Burgess, 1994; Hammer, 1994; Hasson and Mooseker, 1995; Mermall *et al.*, 1998; Mooseker and Cheney, 1995; Titus, 1993).

In comparison to the mammalian and protozoan myosins, little is known about these motors in higher plants (for review see Asada and Collings, 1997; Kendrick-Jones and Reichelt, 1999). The most prominent intracellular motile event depending on the actomyosin cytoskeleton in plant cells is cytoplasmic streaming, i.e. the movement of vesicles and organelles in *Chara* internodal cells and pollen tubes (for review see Kuroda, 1990; McCurdy and Williamson, 1991; Williamson, 1993). In *Chara* cells cytoplasmic streaming occurs at rates of up to 60 $\mu m\,sec^{-1}$ (about an order of magnitude faster than the speed of the fastest muscle) (Kachar and Reese, 1988). A recently isolated myosin protein from *Chara* (Higashi-Fujime *et al.*, 1995; Yamamoto *et al.*, 1995) moves muscle F-actin *in vitro* motility assays at a similar velocity, strongly suggesting that the isolated protein is the motor responsible for cytoplasmic streaming. In Lily pollen tubes (Miller *et al.*, 1995; Tang *et al.*, 1989), and in various tissues from several plants (La Claire, 1991; Qiao *et al.*, 1989; Turkina *et al.*, 1987; Vahey *et al.*, 1982; Yokota *et al.*, 1995), biochemical and immunofluorescence studies using heterologous myosin antibodies have detected myosin-like proteins. Most of these reports demonstrated spot-like anti-myosin labelling throughout the cytoplasm and along actin filaments, and this was interpreted as

Received 19 May 1999; accepted 7 July 1999.
*For correspondence (fax +1223 213 556; e-mail jkj@mrc-lmb.cam.ac.uk).
[†]Present address: Department of Biochemistry, Royal Holloway College, University of London, London TW20 OBE, UK.
[‡]Present address: Department of Biology, University of York, York YO1 5DD, UK.

showing the association of putative myosins with various vesicles and organelles (Grolig *et al.*, 1988; Grolig *et al.*, 1996; Heslop-Harrison and Heslop-Harrison, 1989; Miller *et al.*, 1995). A more recent study has shown heterologous anti-myosin staining associated with plasmodesmata in *Chara* cells (Radford and White, 1998). However, none of these putative myosin proteins has so far been cloned and sequenced to confirm their myosin identity.

The first myosin gene to be cloned and sequenced from a plant, *Arabidopsis thaliana* myosin 1 (ATM1) (Knight and Kendrick-Jones, 1993), was placed by phylogenetic analysis of its motor domain sequence into a new class of myosins (class VIII). Since then a further 10 plant myosin genes (from *Arabidopsis*, *Helianthus*, *Acetabularia* and *Chlamydomonas*) have been cloned and sequenced (Kinkema and Schiefelbein, 1994; Kinkema *et al.*, 1994; La Claire *et al.*, 1995; Vugrek and Menzel, personal communication) and, on the basis of their conserved motor domain sequences, have been placed into three new classes (classes VIII, XI and XIII) (Cope *et al.*, 1996) by phylogenetic analysis. Further analysis of their highly divergent C-terminal tail sequences confirms this classification. None of the plant myosins identified thus far belong to class I or II. The plant myosins in class XI are closely related to the animal myosin Vs but are sufficiently different to be grouped into a separate class (Cope *et al.*, 1996). Furthermore, PCR screens and the *Arabidopsis* genome sequencing project indicate the existence of additional myosins in classes VIII, XI and XIII (Kinkema *et al.*, 1994; La Claire *et al.*, 1995; Moepps *et al.*, 1993; Plazinski *et al.*, 1997; Vugrek and Menzel, personal communication).

The important point to emerge from this analysis is that all the myosin genes identified from plants belong to unique classes which do not contain animal or protozoan myosins. The motile processes in higher plants and animals may be specifically different and, in order to investigate the plant-specific localization and function, we generated an antibody against a recombinant tail region of myosin ATM1. The immunolabelling patterns in root cells from *Lepidium sativum* (cress) and *Zea mays* (maize) indicate that this myosin VIII is predominantly localized at the cell periphery where it is preferentially associated with those plasma membrane regions involved in the assembly of new cell walls. The immunogold and immunofluorescence images reveal that this myosin is also associated with cell-to-cell contact areas in root cells and appears to accumulate specifically in plasmodesmata. These results suggest the intriguing possibility that in plant cells actomyosin-based forces are involved in the selective 'gating' of plasmodesmata.

Results

Immunological studies of myosin VIII in root tissue preparations

To raise antibodies specifically against the *Arabidopsis thaliana* myosin (ATM1), a class VIII plant myosin, we expressed and purified its tail region and used it as the immunogen. This tail region appears to be unique and consists of a short stretch of predicted α-helical coiled-coil (amino acids 950–1019 containing about 10 heptad repeats) and a unique C-terminal region (residues 1020–1166) (Knight and Kendrick-Jones, 1993) which has no apparent homologies or recognisable motifs. The only noticeable features are two clusters of serine residues and a cluster of basic residues at its very C-terminus. For expression, a vector of the pGEX series was modified so that fusion proteins with GST (Glutathione-S-transferase) on their N-termini and a stretch of six histidine residues on their C-termini could be expressed. This vector is especially useful when, as in this case, proteolytic degradation of the expressed protein is a problem. Using the modified vector with two affinity labels, intact fusion protein could be prepared for antibody production.

For our immunological studies, we used root tissue from *Arabidopsis thaliana*, cress (*Lepidium sativum*) and maize (*Zea mays*) and coleoptile tissue from maize for Western blots. Since cress and *Arabidopsis* belong to the same dicot family (*Brassicaceae*), antibodies raised against the *Arabidopsis thaliana* myosin 1 (ATM1) were expected to cross-react with a myosin of the same class in cress and this appears to be the case. We also found that we could obtain the same immunofluorescence pattern in maize roots.

To check the specificity of the affinity-purified polyclonal anti-ATM1 antibody, immmunoblot analyses were carried out on subcellular fractions from cress root and maize coleoptiles (Figure 1). In both cress roots (Figure 1A,a) and maize coleoptiles (Figure 1B,b), the antibody cross-reacts with a 130 kDa band in the microsomal membrane fraction (Figure 1). This subcellular distribution indicates that the intact 130 kDa myosin VIII is associated with the membrane fraction, reminiscent of the membrane localization of the myr 4 myosin in rat brain fractions (Bähler *et al.*, 1994). In our experience, many of the unconventional myosins in animal tissues and tissue culture cells are preferentially bound to cytoskeletal-membrane fractions. In cress roots there is also a faint cross-reacting band at 170 kDa (Figure 1a) which may be the product of one of the class XI myosin genes recently identified by Kinkema and Schiefelbein (1994). When protein extracts were rapidly prepared from cress roots in the presence of a wide spectrum of protease inhibitors and MgATP and subjected to immunoprecipitation with the anti-ATM1 antibody, a single band of approximately 130 kDa was detected on Western blots

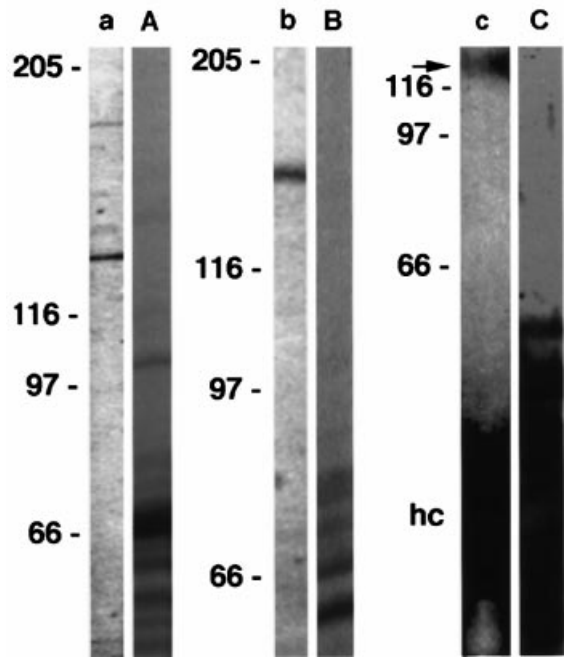

Figure 1. Immunoblot analysis of subcellular fractions of cress root and maize coleoptiles using the anti-ATM1 antibody.
A, B and C are the Coomassie stained SDS-PAGE gels and a, b and c are the corresponding immunoblots. A,a, cress root membrane protein pellet; B,b, maize coleoptile membrane protein pellet; C,c, cress root extract immunoprecipitated with anti-ATM1 antibody (hc = antibody heavy chains (55 kDa) and arrow at 130 kDa = myosin VIII. aA and bB are 5–20% acrylamide gradient gels and cC is a 15% acrylamide gel).

(Figure 1c). The size of the immunoprecipitated protein is in good agreement with the predicted molecular weight of the ATM1 protein (131.2 kDa) (Knight and Kendrick-Jones, 1993). There was no corresponding Coomassie-stained band on the SDS-PAGE gel (Figure 1C) indicating that the amount of myosin VIII in these tissues is likely to be very low. Purified myosin VIII tail fusion protein when mixed with anti-myosin antibody specifically blocked the Western blot and immunofluorescent staining patterns.

Immunolocalization of myosin VIII along the transverse cell walls in root tissue

For the immunolocalization studies, we used root tissue from *Arabidopsis*, cress and maize seedlings. Root tissues were preferred because they are more convenient to handle and their simple architecture allows one to consistently identify the various cell types undergoing different developmental programmes. Virtually identical antibody labelling patterns were obtained with root tissues from all three plants (images from *Arabidopsis* are not shown). Cress and maize roots were preferred: cress because it is closely related to *Arabidopsis* and its roots are more robust, and maize because its cytoskeleton has been comprehensively studied (e.g. Baluska *et al.*, 1992; Blancaflor and Hasenstein, 1995).

The anti-ATM1 antibody strongly labelled the peripheral region underlying the transverse cell walls in the roots of all three plants (Figures 2b,d and 3b). In contrast and acting as an internal control, the longitudinal walls in these cells exhibited rather punctate myosin VIII labelling (Figure 2d,h). The labelling was most prominent in the region containing meristematic and early post-mitotic cells which were undergoing cell division. The strongest labelling was found along newly formed cell walls which were in the process of maturation.

Controls using either pre-immune serum or secondary antibody alone or antibody to vertebrate non-muscle myosin II (Drenckhahn *et al.*, 1983) did not show any staining in root cells (data not shown).

Myosin VIII localisation during mitosis

The distribution of myosin VIII, actin and microtubules during stages in the cell cycle in root meristems in higher plants are shown in Figures 2 and 3 and are summarised in the schematic drawings in Figure 6. At the onset of mitosis (prophase), actin is localised as dense irregular networks surrounding the enlarged, round nucleus (Figures 2a, 3a and 6a). At this stage, myosin VIII labelling is concentrated along the transverse cell walls and is sparsely distributed along the longitudinal cell walls (Figure 2b). At the beginning of metaphase, when the nuclear envelope disintegrates, actin staining is concentrated along the two opposing transverse cell walls with a few actin filaments reaching towards the centre of the cell (Figures 2g and 6b). Myosin VIII labelling is more intense than in prophase and is concentrated at the opposing transverse cell walls, co-localizing with the actin filaments (Figures 2h and 6b).

The different stages in the cell cycle can be readily assigned by following the distribution of microtubules and mitotic chromosomes. At metaphase, when the chromosomes are aligned midway between the spindle poles, dense bundles of kinetochore microtubules connect the chromosomes to the poles (see SP in Figures 3g and 6d). During telophase, in the early phragmoplast (P) region where the new cell wall forms between the separating daughter nuclei, intense anti-tubulin staining is seen as a broad phragmoplast band in the centre of the newly forming cell plate (Figures 3d and 6e). In late cytokinesis, the phragmoplast P* forms a ring-like structure surrounding the newly developing cell plate (Figures 3d,g and 6f). Myosin VIII staining does not occur in the callose-rich cell plate region in the early (P) or in the developing late phragmoplast (P*) (Figures 3c,f and 6f) but is confined entirely to the opposing transverse cell walls which are strongly stained (Figure 3c,f,h). The DAPI-stained chroma-

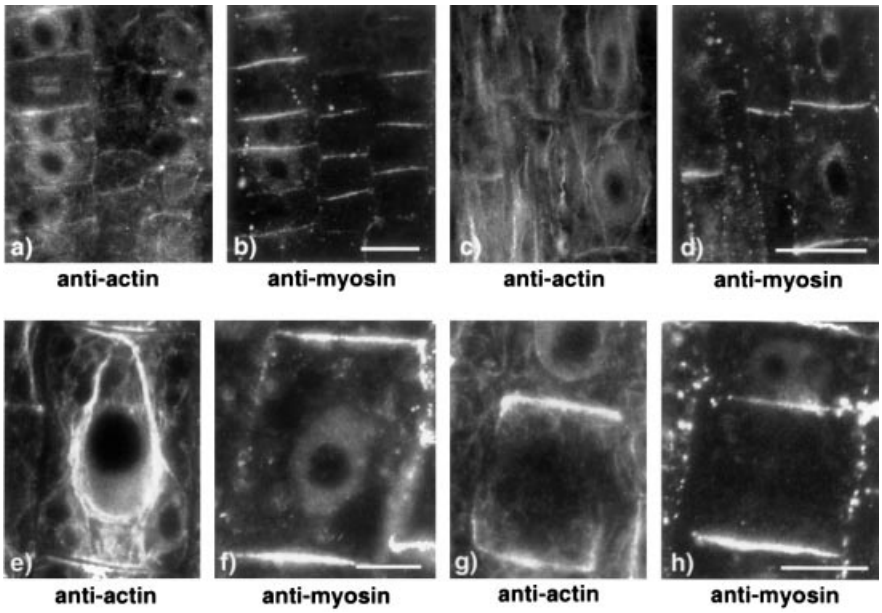

Figure 2. Immunofluorescence localization of myosin VIII and actin in maize root cells.
Cells double-labelled in (a) and (c) with a monoclonal anti-actin antibody and in (b) and (d) with anti-ATM1 antibody. In (e) and (g) root cells stained with the anti-actin antibody are shown and (f) and (h) show cells predicted to be at the same stages stained with the anti-ATM1 antibody. Scale bars in all cases are 10 microns. It was more difficult to obtain the same quality of myosin labelling in myosin/actin compared with tubulin/myosin double labelling because the methanol treatment, which is required for the actin staining, badly affects the myosin staining. Therefore, to demonstrate actin and myosin localization in all cell stages it was necessary to carry out single staining as well as myosin/actin double staining. In (a), smaller isodiametric cells undergoing mitotic division show actin filaments densely concentrated along the transverse cell walls, and in (g) the actin in interphase cells occurs as fine-filamentous networks. In (b), the transverse walls of the root cells are prominently stained with the anti-ATM1 antibody, especially the newly formed walls in G1 stage cells shown in (h) which co-localizes with the actin-staining. In (c) and (e), elongated cells with long actin filament cables traversing the cells are shown; whereas in the same (d) or similar cells (f) only the transverse walls are prominently stained with the anti-ATM1 antibody where it co-localizes with the actin-staining.

tin in these cell stages is still slightly condensed (Figure 3e,i), and the shape and small size of the nuclei reveal that these cells are in a late phase of cell division. Later, in G1-phase (G in Figure 3), shortly after disintegration of the phragmoplast microtubules (Figure 3d,g), extensive labelling of the myosin VIII was detected in this area (Figures 3c,f,h and 6g). In these cells the chromatin in the nuclei is uncondensed (Figure 3e,i), and the phragmoplast microtubules have become integrated into the cortical microtubule network (Figures 3g and 6h). At this late G1 stage, anti-ATM1 staining is thus very strongly concentrated along or in the newly formed cell wall (Figure 3b,f,h) and the actin filaments are arranged in a regular network reaching from the cell walls to the nucleus (Figures 2c,e, 3a and 6c). It should be noted that during all these stages the transverse cell walls are always highly labelled with anti-ATM1 antibody whereas the longitudinal walls show only punctate labelling (Figures 2b,d,h and 3b).

In interphase cells, after completion of cell division, the transverse cell walls are stained with anti-ATM1 antibody, but less brightly than during mitosis (Figure 2d,f). Actin staining of the same region shows a very prominent F-actin array, with characteristically arranged actin filament bundles (Figures 2c,e and 6i). The actin co-localizes with the myosin VIII labelling along the transverse cell walls and extends into the cell centre where the bundles appear to separate into several finer filaments surrounding the nucleus. These finer central actin bundles are not labelled with myosin VIII.

Association of myosin VIII with the plasma membrane and plasmodesmata

1. *Confocal microscopy.* Optical sections through cress root tips labelled with the anti-ATM1 antibody confirmed that the myosin VIII was localized along the whole transverse cell wall, whereas the longitudinal walls show only punctate labelling. An overlay of a phase-contrast image and the fluorescent myosin-staining is shown in pseudo-colour (Figure 4a). The myosin VIII labelling pattern is densely punctate, with the highest density of label in new cell walls in early G1, shortly after phragmoplast disintegration. An overlay of optical sections (Figure 4b) reveals that the punctate labelling pattern passed through the whole cell wall area. Along the longitudinal cell walls a less dense distribution of myosin VIII in distinct patches can also be observed. In Figure 4(c), the myosin VIII labelling in G1-phase cells is shown at a higher

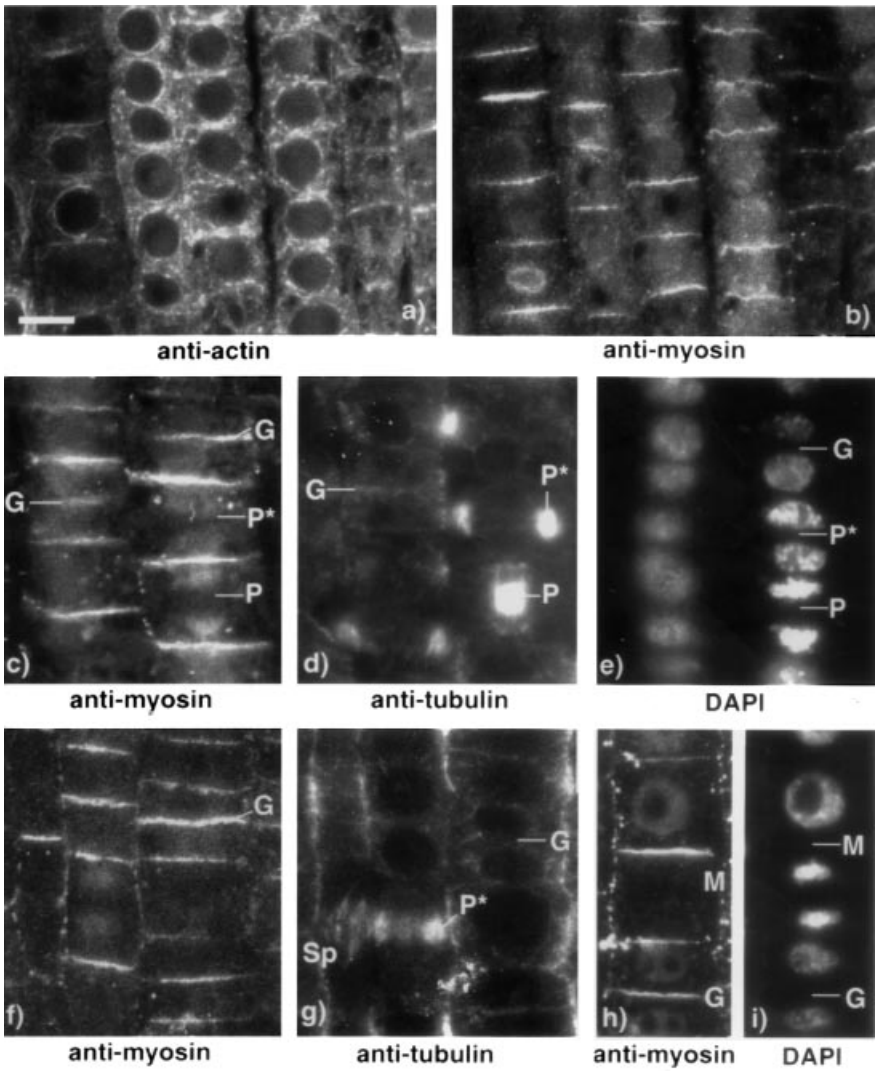

Figure 3. Double-labelling immunofluorescence localization of myosin VIII and actin or tubulin in maize root cells.
Double-labelling of roots cells with (a) anti-actin and (b) anti-myosin. Double-labelling of root cells with (c) anti-myosin, (d) anti-tubulin and (e) DAPI-staining. Cells are in G1-phase (G), early phragmoplast (P) and late phragmoplast (P*) stages. During mitosis the opposing transverse cell walls in early and late phragmoplast stages (P and P*) are specifically labelled with anti-myosin VIII (see c). Cells in early G1-stage (G), recognizible by the smaller size of their nuclei (see e, DAPI-staining), show anti-myosin VIII staining along the newly formed cell wall. Double-labeling of root cells with (f) anti-myosin and (g) anti-tubulin. The mitotic spindle (Sp) and early phragmoplast (P) microtubules are stained with anti-tubulin antibody (see g), but no staining of anti-myosin VIII occurs in the spindle or in the phragmoplast (see g). In the G1-stage (G) cells are strongly stained with anti-myosin VIII along the newly formed cell wall (see f). Double-labeling of root cells with (h) anti-myosin and (i) DAPI-staining. During mitosis in late metaphase (M), the transverse cell walls are strongly stained with anti-myosin VIII. The newly formed cell wall (G) in G1 stages shows strong anti-myosin VIII staining. Scale bar is 10 microns in all micrographs.

magnification, revealing intense myosin VIII labelling of the plasma membrane associated with the newly formed cell wall.

2. *Immunogold electron microscopy.* To confirm these immunofluorescence images, we prepared ultra-thin frozen sections of cress roots and subjected them to indirect immunogold labelling with our anti-ATM1 antibody. In the electron microscope, labelling was detected along the newly formed cell wall between two cells (arrows indicate the 10 nm immunogold particles in Figure 5a,b). This cell wall shows the features of a young cell wall after the disintegration of the phragmoplast and before it loses its 'wavy' appearance, characteristic of the final stages in the maturation of the cell wall. The anti-ATM1/immunogold labelling (10 nm particles) occurred in association with the plasma membrane and at thin membranous structures going through the cell wall which are thought to be plasmodesmata. Other regions of the sections were virtually free of any immunogold labelling.

For a more detailed localisation of the myosin in the cell walls, we used ultra-thin sections of maize roots embedded in LR White Resin which preserves the membrane ultrastructure better than cryo-fixation. Transverse as well as longitudinal cell walls possessing primary and secondary plasmodesmata showed characteristic anti-ATM1/immunogold labelling (Figure 5c,d,e). In young transverse cell walls, plasmodesmata were seen decorated with strings of gold particles (Figure 5c) and in longitudinal cell walls, where secondary plasmodesmata were mostly arranged in large pit fields, the immunogold particles were especially enriched in this area (Figure 5d,e). The cytoplasm and other cell structures were very rarely labelled when compared with the pit fields.

Discussion

We have performed the first cytological characterization of an unconventional myosin in higher plants using an

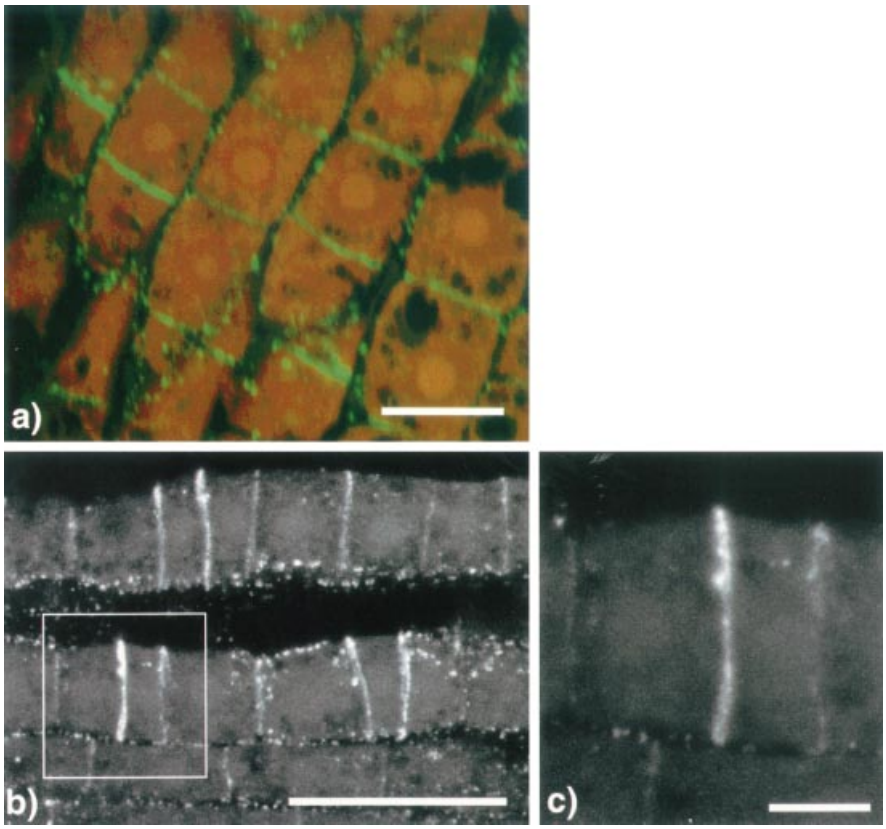

Figure 4. Confocal visualization of cress root cells labeled with anti-myosin VIII antibody. (a) An overlay of a phase-contrast image and immunofluorescent anti-myosin VIII image of cress root sections are shown in false colours, where red is the phase contrast image and green the fluorescence image of myosin VIII staining. The bar is 6 microns. (b) Optical sections through an anti-myosin VIII labelled cress root section. The bar is 10 microns. The region framed in (b) is shown in (c) at higher magnification. The bar is 2.5 microns. An overlay of several optical sections taken in 10 micron steps shows that the transverse cell walls in all growing cells are stained (see b) and cells in G1-phase are especially strongly labelled along the newly formed cell wall (see c).

antibody specifically raised against a recombinant tail region of the first plant myosin gene to be cloned and sequenced. This gene (*ATM1*) was isolated from a dicot plant *Arabidopsis thaliana* (Knight and Kendrick-Jones, 1993). The predicted molecular weight of ATM1 is 131 kDa, and it contains a motor domain (head), four IQ-motifs predicted to bind calmodulin or light chains and a tail domain with a predicted short coiled-coil region which implies its dimerisation into a double-headed molecule. The whole tail region of this myosin was expressed and used as an immunogen to generate specific antibodies. Immunoblot analysis using these anti-ATM1 antibodies identified an approximately 130 kDa band which is highly enriched in the membrane fraction in cress and maize tissues. These results suggest that the myosin VIII is membrane-bound, possibly by its C-terminal globular region. In this connection it is interesting that the animal myosin Is and myosin Vs are known to be bound to membranes (Mooseker and Cheney, 1995).

Immunofluorescence and immunoelectron microscopy of cress and maize root tissues using the anti-ATM1 antibody showed that the myosin VIII is concentrated along the plasma membranes at transverse cell walls both in meristematic cells and in the post-mitotically growing root cells. Cells in G1 phase are extensively stained along their young transverse cell walls, whereas there is only punctate staining along longitudinal cell walls. The immunolocalization patterns show that myosin VIII is concentrated along the transverse walls where F-actin is attached perpendicularly. This suggests that myosin VIII may have some role in the formation of new cell walls as it has a less dense distribution along established side walls. One key feature of the new end walls is that they are a specialized zone of concentrated cell–cell contact where plasmodesmata are formed at cell division. It is significant, therefore, that immunogold studies show myosin to be located at these intercellular plant cell junctions.

In previous studies, myosin-like proteins from plants have been characterized either with cross-reacting antibodies or by stimulation of their ATPase activity by F-actin (for review see Asada and Collings, 1997; Kendrick-Jones and Reichelt, 1999). Such studies have revealed a variety of proteins, perhaps reflecting the diverse classes of myosins. One 240 kDa protein has been isolated from *Chara* that moves muscle F-actin at 60 μm sec^{-1} in *in vitro* motility assays which strongly suggests that this protein is the motor responsible for cytoplasmic streaming. This myosin when viewed in the electron microscope after rotary shadowing (Yamamoto *et al.*, 1995) has similar characteristics to a myosin V, i.e. it is a dimer of two 210–220 kDa heavy chains with pear-shaped heads (motor domains) and a slightly curled globular tail about 80 nm long. Thus far it has not been possible to clone and sequence the gene for this *Chara* myosin. The predicted molecular weights of

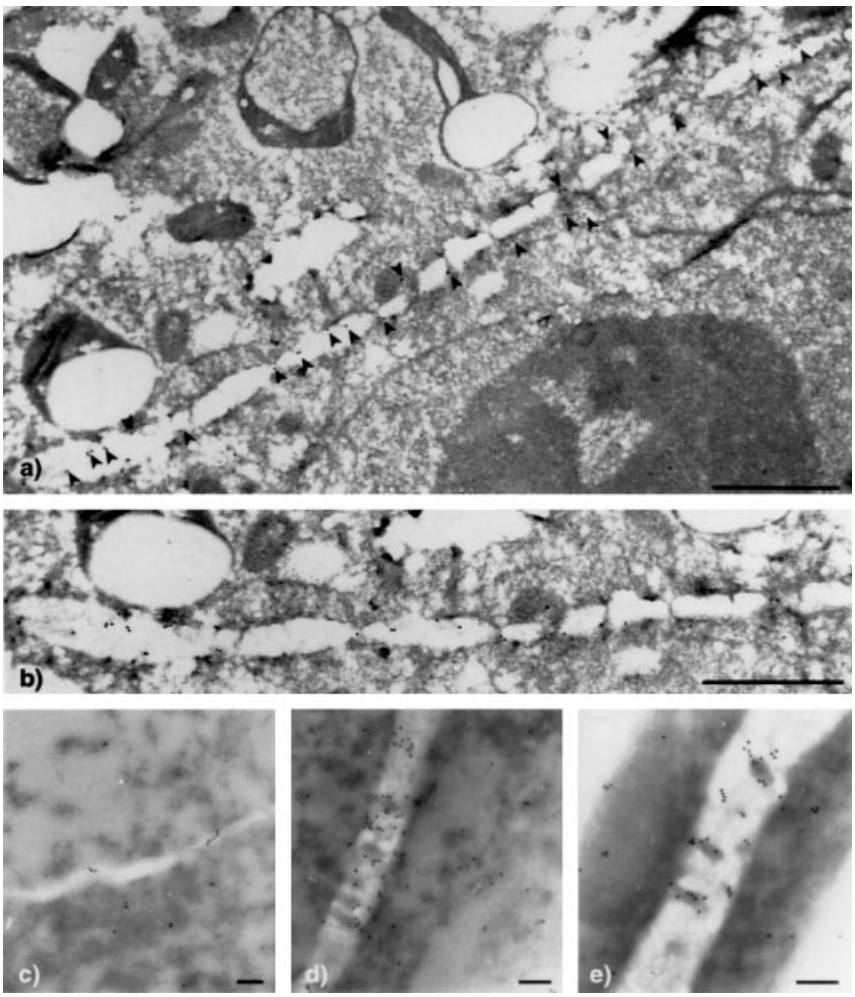

Figure 5. Immunoelectronmicroscopic localization of myosin VIII in cress roots.
(a) The cell wall in the centre of this micrograph shows the features of a 'fenestrated sheet' structure indicating a young cell wall after the disintegration of the phragmoplast and before the cell wall loses its 'wavy' structure, indicating the increasing deposit of cellulose and cell matrix components. The 10 nm immuno-gold/anti-ATM1 antibody particles (arrowheads) occur associated with the plasma membrane of the new cell wall and at thin membranous structures and plasmodesmata going through the wall. Other regions of the sections were virtually free of any gold particles. Scale bar is 1 micron. (b) The new cell wall is shown at a higher magnification, scale bar is 1.5 microns. (c) A recently formed transverse cross-wall in a cortical cell from the basal part of the meristem. The immuno-gold particles decorate the primary plasmodesmata formed during cytokinesis. (D) A longitudinal section through a cell wall in a cortical cell from the transition region. Note the massive accumulation of immuno-gold particles in secondary plasmodesmata organized into pit-fields. (e) A longitudinal section through a cell wall in a cortical cell from the apical part of the elongation region. Immuno-gold particles are prominently associated with pit-fields. Scale bars for Figure 5(c,d,e) are 0.5 microns.

class VIII myosins is about 130 kDa and for class XI myosins about 170 kDa. In higher plants, a 170 kDa myosin has been biochemically isolated from lily pollen tubes (Yokota and Shimmen, 1994) and an antibody to this protein recognizes 170 kDa polypeptides in tobacco, *Tradescantia* and *Arabidopsis* tissue (Yokota *et al.*, 1995). When heterologous anti-myosin antibodies have been used to stain plant cells, they have mostly produced punctate staining patterns throughout the cell which is indicative of the labelling of organelles and vesicles involved in membrane transport (Grolig *et al.*, 1988; Miller *et al.*, 1995; Qiao *et al.*, 1989). It can be concluded that homologues of the myosin superfamily exist in higher plants and are involved in a variety of membrane associated processes. However, it is clear that the anti-myosin VIII localization reported here has distinct differences from these previous studies. One of the striking features of myosin VIII localization is that it becomes concentrated in newly deposited cross-walls in contrast to its sparse occurrence along side walls. This suggests that it may be involved, not so much in the process of vesicle transport and fusion which bring cell plate precursors to the mid-line of the phragmoplast, but in those processes of cell plate maturation. Indeed, myosin VIII labelling is found most strongly when the actin and microtubules of the phragmoplast have depolymerized, and it is important to examine the stage-specific processes in which myosin VIII may be implicated.

Several studies show that cell wall formation occurs in two separate stages. For instance, caffeine is known not to effect the formation of the phragmoplast cytoskeleton nor the actual deposition of the central cell plate, but the later stage of fusion with the mother wall and the conversion of the callose-rich plate into a less flexible wall (Hepler and Bonsignore, 1990; Valster and Hepler, 1997). Mineyuki and Gunning (1990) have reviewed these later stages of cell division and concluded that insertion and maturation factors interact with the cell plate or pass into it from the cortical division site. Callose (a major component of the cell plate) is removed from cell plates soon after they attach (Northcote, 1989) and pectic polysaccharides are inserted (Moore and Staehelin, 1988; Samuels *et al.*, 1995).

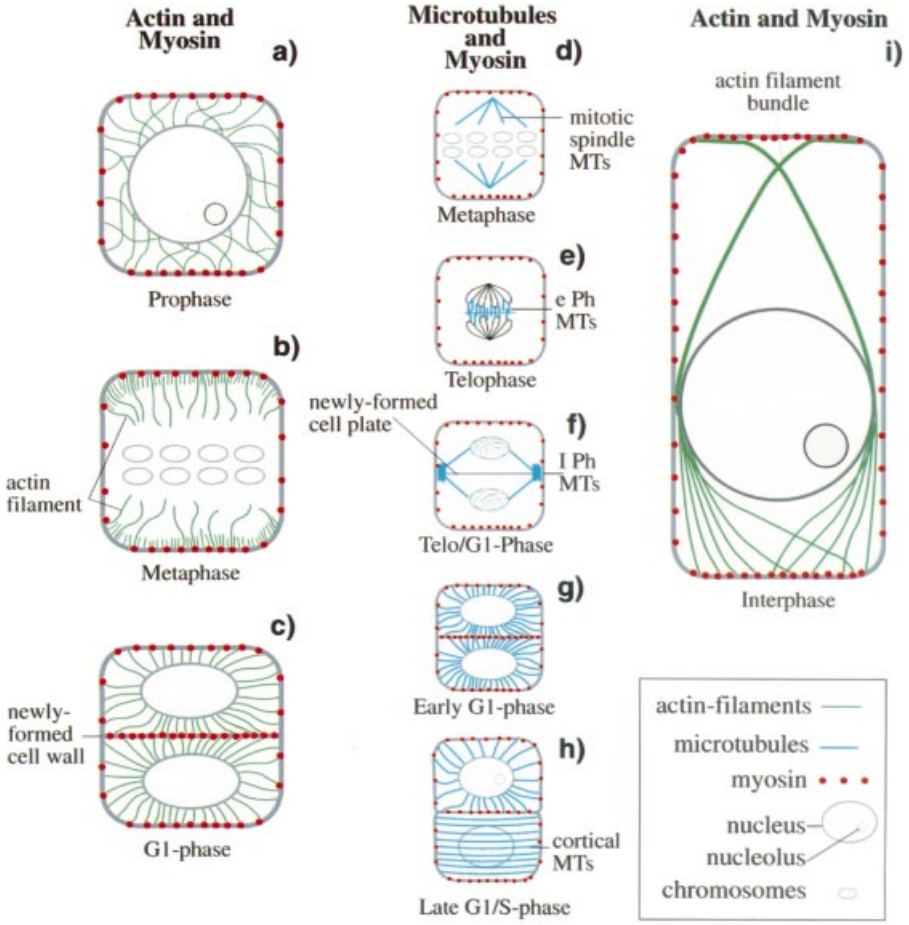

Figure 6. Schematic drawings of the distribution of myosin VIII, actin filaments and microtubules in cells of the meristem and transition growth zone in the root apex.

Cell walls and the underlying plasma membrane are represented as one grey line. The drawings represent the distribution of the cytoskeletal elements in the median level of the cells, only in late G1/S-phase are cortical microtubules shown (as indicated). (a) In prophase, actin filaments are distributed as dense irregular networks surrounding the enlarged round nucleus (Figure 2a). Myosin VIII labelling is concentrated along the transverse cell walls and sparsely distributed along the longitudinal cell walls (Figure 2b,d). (b) In metaphase, the nuclear envelope disintegrates and the chromosomes are arranged along the equatorial plane. The F-actin at this stage forms a dense network of short filaments on the two opposing transverse cell walls with a few actin filaments reaching towards the cell centre, but not into the equatorial plane (Figure 2g). Myosin VIII labelling is more dense than in prophase, concentrated at the opposing cell walls, co-localizing with actin (Figure 2h). (c) In G1-phase, the newly formed plasma membrane and cell wall separates the daughter cells. Actin filaments are arranged in a regular network reaching from the cell walls to the nucleus (Figure 2e). The highest density of myosin VIII labelling is located along the newly assembled cell wall (Figure 2d). The transverse cell walls are also strongly labelled with ATM1 antibody whereas the longitudinal walls show only weak punctate labelling. The different cell cycle stages can be identified by the distribution of microtubules and the chromosomes. (d) At metaphase, when the chromosomes are aligned midway between the spindle poles, dense bundles of microtubules connect the chromosomes to the pole (Figure 3g). (e) After separation of the chromosomes into daughter nuclei in late telophase, microtubules of the early phragmoplast (P-MTs) are concentrated between the separating nuclei (Figure 3d).At this stage, numerous Golgi-derived vesicles accumulate at the equatorial plate to initiate cell plate formation. (f) During late telophase/G1-phase, the late phragmoplast microtubules (P*-MTs) are concentrated as a ringlike-structure surrounding the leading edges of the assembling cell plate (Figure 3d,g). Additional vesicles fuse with the phragmoplast, extending it outwards and eventually the phragmoplast fuses with the plasma membrane, and the two cells separate. In (d–f) no myosin VIII staining was observed in the mitotic spindle during the separation of the chromosomes or in the early or late phragmoplast (Figure 3c,f). However, the opposing transverse cells walls are strongly stained with myosin VIII during these stages in the cell cycle, co-localizing with actin filaments during metaphase. (g) In early G1-cells, after phragmoplast disintegration and cell plate assembly, the ATM1 labelling becomes concentrated along the newly formed cell wall which separates the daughter cells (Figure 3b,c). (h) Later in G1-phase, when the nuclear membranes have completely reformed around each daughter nucleus and the nucleoli are visible (Figure 3e,i), the microtubules and the actin are arranged as dense networks interconnecting the centrally located nucleus with the cell periphery. At this stage, the highest density of ATM1 labelling is located along the newly assembled cell wall (Figure 3c). (i) During interphase, when the root cells elongate, the actin filaments are extending from perinuclear sites towards the opposite transverse walls of the cell where they co-localize with the myosin VIII (only two actin bundles in the median level are shown) (Figure 2c,d). These actin filaments may form a transport pathway for Golgi-derived vesicles carrying new cell wall components.

The appearance of myosin VIII coincides therefore with the onset of these wall-consolidating processes. The protein could bring the islands of membrane plate material together or it could trigger the exocytosis of new cell wall material. High concentrations of calcium–calmodulin are found near the phragmoplast/cell plate (Hepler, 1994) and

it is possible that changes in the calcium levels at the transition between plate deposition/maturation affect the localisation and activity of myosin VIII. In *Chara*, a polyclonal antibody raised against smooth and skeletal myosin has been shown to label plasmodesmata (Radford and White, 1998) – a localisation pattern which agrees with our previous results (Reichelt *et al.*, 1997) and this paper.

In the early post-mitotic root cells of cress and maize the transverse walls are intensely labelled with the anti-myosin VIII and actin antibodies. This myosin antibody does not decorate F-actin cables involved in cytoplasmic streaming but it is interesting that myosin VIII is concentrated along those walls to which the longitudinal actin cables are directed and attached. The cytoplasmic actin cables largely depolymerize in cell division but streaming is restored along the interphase array during early postcytokinesis. Another possible role for myosin VIII (which is detected in the membrane fraction) is that it may be part of the system for anchoring or directing the cytoplasmic F-actin cables. Since F-actin goes to (or through) plasmodesmata (White *et al.*, 1994), it has been suggested to be involved in the intercellular movement of certain viruses (McLean *et al.*, 1995), proteins and mRNA (Lucas *et al.*, 1996). Such particle movement is most likely to be an exaggerated form of normal directed cell transport. It is interesting therefore that the density of plasmodesmata is far greater in the transverse end walls than in the longitudinal side walls (Juniper and Barlow, 1969). The movement of virus particles (McLean *et al.*, 1995; Waigmann and Zambryski, 1995; Zambryski, 1995), and the fact that cytochalasin D enlarges the plasmodesmatal neck (White *et al.*, 1994), indicates that there is a gating mechanism which controls the size of the pore and that this is likely to be under contractile regulation (Ding *et al.*, 1996; Overall *et al.*, 1982; White *et al.*, 1994). The present study has shown that myosin VIII is localized at plasmodesmata and, particularly since it is an actin-interacting protein, is a strong candidate for being part of any intercellular gating complex.

Experimental procedures

Materials

Analytical grade reagents were obtained from BDH Chemicals Ltd (Poole, UK), Bethesda Research Laboratories Inc. (Gaithersburg, MD, USA) and Sigma Chemical Co. Ltd (Poole, UK). Enzymes supplied by New England BioLabs (Hertfordshire, UK) and Promega Corporation (Madison, WI, USA) were used according to the manufacturer's standard assay conditions. Radiochemicals were supplied by Amersham International (Amersham, UK). Oligonucleotides were synthesized on an Applied Biosystems 390B automated synthesizer (Applied Biosystems Inc., Foster City, CA, USA) by Terry Smith (Laboratory of Molecular Biology, Cambridge, UK).

Expression of recombinant ATM1 and antibody preparation

The vector pGEX-H6 used for the expression of the tail region of *Arabidopsis thaliana* myosin VIII (ATM1) is based on pGEX4T-3 (Pharmacia) with the addition of a C-terminal string of six histidine residues. This allows the intact expressed protein to be purified using two specific affinity tags by the so-called 'affinity-sandwich' protocol (Binder *et al.*, 1994). The vector was constructed by inserting a double-stranded oligonucleotide consisting of: 5′-GGC CGC CAC CAT CAC CAT CAC CAT –3′ and 5′-GGC CAT GGT GAT GGT GAT GGT GGC–3′ into the *Not*I site of pGEX4T-3. This oligonucleotide introduces the 6 His (H6) sequence C-terminal to a regenerated *Not*I site such that if the insert is correctly engineered this His-tag should remain in frame with both upstream sequences and the downstream stop codon.

The ATM1 insert was produced by PCR using the intact ATM1 cDNA clone (3.851Kb) (Knight and Kendrick-Jones, 1993) as template and the following oligonucleotides: 5′-CGA ATT CCC GGG TCG GAG GTG CCA AGA CAA ATG AGT TAG GTG AG–3′ and 5′-GCC ACG ATG CGG CCG CTA TAC CTG GTG CTA TTT CTC CTT CCC CAC CA–3′ as primers which also introduce *Not*I and *Xma*I restriction sites (underlined). The PCR product (2952–3632 in the ATM1 cDNA) containing the whole tail-region of ATM1 including the coiled-coil and the C-terminal globular regions (amino acid residues 938–1166) was first blunt-end cloned into puc18, digested with *Hinc*II and transformed into *E. coli* JM101 cells. Positive clones were recognized by blue/white selection and PCR screening and were sequenced. Clones which contained the correct inserts were digested with *Not*I and *Xma*I and ligated into the dephosphorylated expression vector pGEX-H6. The ATM1-pGEX-H6 construct was expressed in *E. coli* BL21 (DE3) cells (Studier and Moffat, 1986). Freshly transformed colonies were inoculated into 2XTY medium containing 100 mg ml^{-1} ampicillin, grown overnight at 37°C and then induced with 0.6 mM IPTG and grown for a further 3 h at 37°C. The cells were harvested by centrifugation at 5000 ***g*** and resuspended in PBS containing 1% TritonX-100 and a battery of protease inhibitors (see section on immunoprecipitation and Western blot analysis). The cells were lysed in a French Press and the supernatant collected by centrifugation at 12 000 ***g***. The ATM1 was expressed as a soluble fusion protein, GST-ATM1-H6, with a molecular weight of 54 kDa. The supernatant was filtered through a 0.45 μm filter and applied to a Glutathione(GT)-Sepharose 4B column and purified according to the manufacturer's instructions (Pharmacia P-L Biochemicals Inc.). After application of the expressed protein, the GT-Sepharose column was washed with at least four volumes (volume of supernatant applied) of PBS containing 1% Triton X-100 and the protease inhibitor cocktail and the bound fusion protein eluted with 10 mM glutathione, 50 mM Tris–HCl, pH 8.0. Further purification of the fusion protein using the His-tag by Ni-affinity chromatography was performed under non-denaturing conditions according to the manufacturer's instructions (Novagen, Inc.).

The ATM1-GST fusion protein was further purified by SDS-PAGE on a 10% acrylamide maxi-gel and the major band cut out and electroeluted. Three 100 μg aliquots of this fusion protein were used for antibody production in rabbits, as described by Harlow and Lane (1988). The resulting polyclonal serum was affinity-purified for the localization and Western blotting studies in two steps; first using a glutathione-S-transferase (GST)-agarose affinity column to remove any anti-GST antibodies and then using the recombinant ATM1 protein on immunoblots to purify the anti-ATM1 antibodies. For these immunoblots the recombinant

protein purified on a GT-Sepharose column was separated on an SDS-Page gel and transferred to nitrocellulose. The nitrocellulose blot was stained with Ponceau red and the strips containing the recombinant ATM1 were cut out, blocked with 5% non-fat dry milk in TBS (Tris buffered saline) for 1 h and then incubated with the undiluted polyclonal serum overnight at 4°C on a rotating wheel. The nitrocellulose strips were washed repeatedly with TBS containing 0.05% Tween 20 and the bound ATM1-antibodies eluted by vortexing the strips for 30 sec in 0.2 M Glycine, pH 2.2, and then quickly neutralizing with 1 M Tris–HCl, pH 7.6. The specificity of these purified antibodies was checked on blots; they strongly cross-reacted against GST-ATM1 fusion protein and thrombin cleaved 28 kDa fragment (see below) but gave no reactivity against GST even at low dilution. These antibodies weakly cross-react with the tail regions of purified chicken skeletal and brush border cytoplasmic myosin IIs. To check the identity of the expressed GST-ATM1 fusion protein it was cleaved with thrombin to yield 26 kDa and 28 kDa fragments. N-terminal sequencing of the 28 kDa fragment confirmed that it was the tail region of ATM1 and the commercially available anti-GST antibody (Pharmacia P-L Biochemicals Inc.) identified the 26 kDa fragment as GST.

For competitive blocking of the anti-ATM1 antibodies, soluble myosin VIII tail fusion protein was expressed and purified using Ni^{2+}-NTA-Agarose chromatography (Qiagen Ltd) in PBS.

Immunoprecipitation, subcellular fractionation and Western blot analysis

To detect the ATM1 protein in cells by immunoprecipitation, fresh 2-day-old cress roots were homogenized in an ice-cold solution containing 0.2 M KCl, 15 mM Tris–HCl, ph 7.2, 1 mM EDTA, 5 mM DTT, 0.1% Triton X-100, and a broad range of protease inhibitors (10 μg ml^{-1} aprotinin, 10 μg ml^{-1} chick ovalbumin trypsin inhibitor, 10 μg ml^{-1} N-benzoyl-L-arginine ethyl ester hydrochloride (BAEE), 10 μg ml^{-1} tosyl-L-arginine methyl ester (TAME), 0.1 mM phenylmethylsulphonyl fluoride (PMSF), 10 μg ml^{-1} pepstatin, 10 μg ml^{-1} leupeptin (all obtained from Sigma) and 0.5 mM Pefabloc SC (AEBSF) 4-(2-Aminoethyl)-benzenesulphonyl fluoride (Boehringer, Mannheim, Germany). The roots were first homogenized in a Polytron Omnimixer (Kinematica, Luzern, Switzerland), then in a Dounce homogenizer and the cell debris removed by filtration through one layer of nylon mesh. ATP and $MgCl_2$ were added to the preparation to a final concentration of 5 mM and 10 mM, respectively, and the cells lysed in a French press under high pressure. A further aliquot of 5 mM MgATP was added, and the preparation immediately centrifuged at 50 000 ***g*** for 30 min. Two millilitres of the supernatant was incubated with 100 μl anti-ATM1 antibody for 1 h at 4°C and then 50 μl of Protein-A-Sepharose CL-4B (Sigma, P-3391) (swollen in PBS) was added and incubated for a further 1 h at 4°C. The immunocomplexes bound to the protein-A-beads were washed three times with 2 ml of PBS and then finally drained with a syringe inserted directly into the beads to completely remove the PBS. For SDS-PAGE (Matsudeira and Burgess, 1978), 50 μl of sample buffer (2%SDS, 10% glycerol, 100mMDTT, 60mMTris–HCl, pH 6.8 and 0.001% bromphenol blue) was added to the beads, heated to 85°C for 5 min, centrifuged and the supernatant loaded onto a gel.

The protein samples were run on SDS-PAGE 5–20% acrylamide gradient gels using the method of Matsudaira and Burgess (1978) and electrophoretically transferred to 0.1 μm nitrocellulose (Schleicher & Schuell, Dassel, Germany) according to the method of Burnette (1981). The nitrocellulose was blocked with 10% (w/v) Marvel (non-fat dry milk) in PBS containing 0.3% Tween-20 (blocking buffer) before incubating with the anti-ATM1 antibody diluted 1 : 500 in blocking buffer. The secondary antibody was biotinylated goat anti-rabbit IgG(H + l) Vectastain, diluted 1 : 200 and the blot developed using the Vectastain ABC Peroxidase kit (PK-4001, Vector Laboratories, Peterborough, UK). Developing solution was 0.9 mg ml^{-1} DAB, 0.4 mg ml^{-1} $NiCl_2$, 0.01%H_2O_2 in 100 mM Tris, pH 7.5.

To prepare fractions containing the membrane bound proteins, plant material (cell cultures from Arabidopsis, cress roots and maize coleoptiles) was homogenized (10 min in a mortar) in an ice-cold solution of 250 mM Tris–HCl (pH 8.0), 25 mM EDTA, 330 mM sucrose, 5 mM DTT, 5 mM ascorbic acid and 1 mM phenyl-methylsulphonyl fluoride (PMSF) followed by filtration through one layer of nylon mesh. All subsequent steps were carried out at 4°C. The post-mitochondrial supernatant (15 min, 4000 g; Biofuge 22R-Heraeus, Offenbach, Germany) was centrifuged for 50 min at 13 800 ***g*** (Biofuge 22R-Heraeus). The resulting pellet was used as the membrane bound protein fraction. For Bradford analysis the latter sample was resuspended in 200 μl of a solution containing 10 mM MES/bis-tris-phosphate (BTP) pH 7.5, 5 mM EDTA and 20% glycerol.

SDS-PAGE was performed on these samples diluted in sample buffer containing 3% SDS, 6% sucrose, 100 mM DTT, 60mMTris–HCl, pH 6.8, and 0.001% bromphenol blue. The samples were heated to 80°C for 10 min, centrifuged and the supernatant loaded onto 8% gels. After protein separation, the gels were stained with Coomassie blue or electrophoretically transferred to nitrocellulose using a transblot cell (Bio-Rad, München, Germany). For immunostaining (at room temperature) the nitrocellulose membrane was pre-incubated with 4% BSA in TBS for 30 min, washed for 30 min (three times for 10 min) in TTBS (TBS buffer containing 0.05% Tween-20) and incubated with anti-ATM1 antibody (diluted 1: 1000 in TTBS; control in TTBS). After washing in TTBS the membrane was incubated for 1 h in TTBS containing the secondary antibody (goat anti-rabbit IgG, whole molecule) conjugated to alkaline phosphatase (Sigma A-9919; dilution 1: 100 000). Washing in TTBS was followed by alkaline phosphatase detection using the fast-red staining protocol described by Druguet and Pepys (1977).

Immunofluorescence and immunogold localization of ATM1

The specimens for immunofluorescence microscopy were prepared by the method of Baluska *et al.* (1992). Briefly, 2-day-old cress and maize roots were cut and fixed in 4% formaldehyde in MTSB (Microtuble Stabilizing Buffer) containing 50 mM PIPES, 5 mM $MgSO_4$ and 5 mM EGTA, pH 6.9 for 1 h at room temperature. The roots were dehydrated in a graded ethanol series (30% to 97% ethanol in PBS) (PBS contained 0.14 M NaCl, 2.7 mM KCl, 6.5 mM Na_2HPO_4, 1.5mMK_2HPO_4, 3 mM NaN_3, pH 7.3) then incubated in wax:ethanol (1 : 2, 1 : 1 and 2 : 1 steps) and finally infiltrated in 100% Steedman's wax (PEG-400 distearate and 1-hexadecanol, 9 : 1(w/w)) at 37°C. The infiltrated roots were then embedded by allowing the wax to polymerize at room temperature. Longitudinal sections 4 μm thick were cut with a microtome (Jung, Heidelberg, Germany) and mounted on slides coated with glycerol-albumen (Serva). The sections were dewaxed in 100% ethanol, rehydrated in an ethanol series (97% to 30% ethanol in PBS), washed with PBS and then finally with MTSB. If sections were subjected to immunostaining with anti-actin antibody, incubation in methanol at –20°C for 10 min was required after

the ethanol series (Vitha *et al.*, 1997). After methanol, the sections were washed with PBS and then MTBS. For immunostaining the sections were incubated with the affinity-purified anti-ATM1 antibody (diluted 1 : 200 in PBS with 0.1% BSA) or monoclonal anti-actin (ICN, anti-actin, clone C4, cat. no. 69–100) or anti a-tubulin antibody (Amersham, N356) (both diluted 1 : 200 in PBS-BSA) for 60 min at room temperature. After washing with MTSB, the sections were incubated with fluorescein isothiocyanate (FITC) conjugated anti-rabbit IgG raised in goat (Sigma Chemical Co, St. Louis, MO, USA, F-6005) or rhodamine-conjugated anti-mouse IgG raised in goat (Sigma, T-5393), both diluted 1 : 200 in PBS-BSA, for 1 h at room temperature. Controls included incubating with secondary antibody only, mouse pre-immune serum and monoclonal anti-thymus-myosin II antibody which cross-reacts against a wide spectrum of cytoplasmic myosin IIs in animal cells (Drenckhahn *et al.*, 1983). DNA was labelled by incubating with DAPI (10 μg ml^{-1}) for 5 min at room temperature. Specimens were examined in a Zeiss Axiovert using a Zeiss Planachromat or Neofluar 40× or 100×. Micrographs were taken using Kodak Ektachrome 400 ASA film. The labelled sections were also viewed in a confocal laser scanning microscope (Bio-Rad MRC 600) equipped with argon/krypton lasers and dual excitation/emission filter sets for both TRITC and FITC for the double-labelled specimens.

For immunoelectron microscopy 2-day-old cress roots were cut and fixed in 8% formaldehyde and 0.1% glutaraldehyde in PBS for 1 h at room temperature, embedded in a drop of 3.2 M sucrose and frozen on metal holders in liquid nitrogen. Ultra-thin sections were cut on an cryo-ultramicrotome (Ultracut UCT, Leica/Reichert-Jung, Germany) fitted with cryodevice FC-S and transferred onto nickel grids. The sections were blocked against non-specific labelling by incubating in 0.02 M glycine in PBS for 10 min, 2% gelatin in PBS for 5 min and 0.1% BSA (typeV, Sigma) +5% FCS in PBS for 10 min. For immunolabelling the sections were incubated at room temperature for 30 min with the primary antibody, affinity-purified anti-ATM1 (diluted 1 : 50 in PBS/BSA). They were washed with PBS/BSA and then incubated with secondary antibody goat antirabbit IgG-10 nm gold conjugate (BioCell, Cardiff, U.K) diluted 1 : 50 in PBS/BSA. The sections were washed with PBS and the reaction stabilized with 1% glutaraldehyde in PBS. After washing in distilled water, sections were contrasted with ice-cold 0.4% uranyl acetate in 1.8% methylcellulose. Labelled sections were examined in a Philips EM301 electron microscope at 80 kV.

For the immunolocalisation studies on plasmodesmata (Figure 5c,d,e) a similar protocol was used. Two-day-old maize roots were cut and fixed in 4% paraformaldehyde in MTSB buffer for 90 min at room temperature. After washing in MTSB and PBS, and dehydration in a graded ethanol series, the tissue was embedded in LR White Resin (Hard grade, Biocell, Cardiff, UK) and left to polymerise at 36°C. Ultra-thin sections were cut on an ultramicrotome and transferred onto formvar coated nickel grids. The sections were blocked with 50 mM glycine, 5% BSA and 5% normal goat serum in PBS for 30 min and washed with wash buffer (WB) (PBS containing 1% BSA and 0.1% gelatin). They were incubated first with anti-ATM1 (diluted 1 : 50 with WB) at room temperature for 90 min, washed with WB and incubated with the second antibody, goat anti-rabbit IgG-10 nm gold conjugate (diluted 1 : 50 in WB) for 90 min. The sections were washed with WB and PBS, post-fixed with 3% glutaraldehyde for 15 min, washed extensively with distilled water and contrasted with ice-cold 2% aqueous uranyl acetate and 1% osmium tetroxide (to enhance plasmodesmata visualization). The labelled sections were examined in a Zeiss EM 10 electron microscope at 60 kV.

Acknowledgements

We wish to thank Drs Paul Luzio and Nick Bright (Department of Clinical Biochemistry, University of Cambridge) for the use of their facilities and for advice and assistance with the immunoelectron microscopy; Pat Edwards and Dr Brad Amos for their help with the confocal microscopy; Dr Jamie Cope for his advice on the molecular biological aspects of this work; and Monika Polsakiewicz for excellent technical assistance. This work was supported by fellowships to S.R. from Graduiertenförderung des Landes Nordrhein-Westfalen, Deutscher Akademische Austauschdienst (DAAD) and Boehringer Ingelheim Fonds. Financial support to AGRAVIS (Bonn) by the Deutsche Agentur für Raumfahrtangelegenheiten (DARA, Bonn) and the Ministerium für Wissenschaft und Forschung (MWF, Düsseldorf) is gratefully acknowledged.

References

Asada, T. and Collings, D. (1997) Molecular motors in higher plants. *Trends Plant Science*, **2**, 29–37.

Bähler, M. (1996) Myosins on the move to signal transduction. *Curr. Opin. Cell Biol.* **8**, 18–22.

Bähler, M., Kroschewski, R., Stoffler, H.-E. and Behrmann, T. (1994) Rat myr4 defines a novel class of myosin I: identification, distribution, localisation and mapping of calmodulin binding sites with differential calcium sensitivity. *J. Cell Biol.* **126**, 375–389.

Baluska, F., Parker, J.S. and Barlow, P.W. (1992) Specific patterns of cortical and endoplasmic microtubules associated with cell growth Rearrangements of F-actin arrays in growing cells of intact maize root apex tissues: a major developmental switch occurs in the postmitotic transition region. *Eur. J. Cell Biol.* **72**, 113–121.

Binder, B.M., Harper, J.F. and Sussman, M.R. (1994) Characterization of an Arabidopsis calmodulin-like domain protein kinase purified from *Escherichia coli* using an affinity sandwich technique. *Biochemistry,* **33,** 2033–2041.

Blancaflor, E. and Hasenstein, K.H. (1995) Growth and microtubule orientation of maize roots subjected to osmotic stress. *Int. J. Plant Sci.* **156**, 794–802.

Burnette, W.N. (1981) 'Western blotting': Electrophoretic transfer of proteins from sodium dodecyl sulfate-polyacrylamide gels to unmodified nitrocellulose and radiographic detection with antibody and radioiodinated protein A. *Anal. Biochem.* **112**, 195–203.

Cope, M.J.T.V., Whisstock, J., Rayment, I. and Kendrick-Jones, J. (1996) Conservation within the motor domain: Implications for structure and function. *Structure*, **4**, 969–987.

Ding, B., Kwon, M.-O. and Warnberg, L. (1996). Evidence that actin filaments are involved in controlling the permeability of plasmodesmata in tobacco mesophyll. *Plant J.* **10**, 157–164.

Drenckhahn, D., Groeschel-Stewart, U., Kendrick-Jones, J. and Scholey, J.M. (1983) Antibody to thymus myosin: Its immunological characterization and use for immunocytochemical localization of myosin in vertebrate nonmuscle cells. *Eur. J. Cell Biol.* **30**, 100–111.

Druguet, M. and Pepys, M.B. (1977) Enumeration of lymphocyte populations in whole peripheral blood with alkaline phosphatase-labelled reagents. A method for routine clinical use. *Clin. Exp. Immunol.* **29**, 162–167.

Fath, K.R. and Burgess, D.R. (1994) Membrane motility mediated by unconventional myosin. *Curr. Opin. Cell Biol.* **6**, 131–135.

Grolig, F., Schroeder, J., Sawitzky, H. and Lange, U. (1996) Partial characterization of a putative 110 kDa myosin from the green

alga Chara corallina by in vitro binding of fluorescent F-actin. *Cell Biol. Int.* **20**, 365–373.

Grolig, F., Williamson, R.E., Parke, J., Miller, C. and Anderton, B.H. (1988) Myosin and Ca^{2+}-sensitive streaming in the alga *Chara*: detection of two polypeptides reacting with a monoclonal anti-myosin and their localization in the streaming cytoplasm. *Eur. J. Cell. Biol.* **47**, 22–31.

Hammer, J.A., III (1994) The structure and function of unconventional myosins: a review. *J. Muscle Res. Cell Motil.* **15**, 1–10.

Harlow, E. and Lane, D. (1988) *Antibodies: A Laboratory Manual.* Cold Spring Harbor: Cold Spring Harbour Laboratory Press.

Hasson, T. and Mooseker, M.S. (1995) Molecular motors, membrane movements and physiology: Emerging roles for myosins. *Curr. Opin. Cell Biol.* **7**, 587–594.

Hepler, P.K. (1994) The role of calcium in cell division. *Cell Calcium*, **16**, 322–330.

Hepler, P.K. and Bonsignore, C.L. (1990) Caffeine inhibition of cytokinesis: Ultrastructure of cell plate formation/degradation. *Protoplasma*, **157**, 182–192.

Heslop-Harrison, J. and Heslop-Harrison, Y. (1989) Myosin associated with the surface of organelles, vegetative nuclei and generative cells in angiosperm pollen grains and tubes. *J. Cell Sci.* **94**, 319–325.

Higashi-Fujime, S., Ishikawa, R., Iwasawa, H., Kagami, O., Kurimoto, E., Kohama, K. and Hozumi, T. (1995) The fastest actin-based motor protein from the green algae, *Chara*, and its distinct mode of interaction with actin. *FEBS Lett.* **375**, 151–154.

Juniper, B.E. and Barlow, P.W. (1969) The distribution of plasmodesmata in the root tip of maize. *Planta*, **89**, 352–360.

Kachar, B. and Reese, T.S. (1988) The mechanism of cytoplasmic streaming in *Characean* algal cells: Sliding of endoplasmic reticulum along actin filaments. *J. Cell Biol.* **106**, 1545–1552.

Kendrick-Jones, J. and Reichelt, S. (1999) Myosin, plant. In *The Guidebook of Cytoskeletal and Motor Proteins* 2nd Edn (Kreiss, T. and Vale, R., eds). Oxford: Oxford University Press, pp. 457–460.

Kinkema, M. and Schiefelbein, J.W. (1994) A myosin from a higher plant has structural similarities to class V myosins. *J. Mol. Biol.* **239**, 591–597.

Kinkema, M., Wang, H. and Schiefelbein, J.W. (1994) Molecular analysis of the myosin gene family in *Arabidopsis thaliana. Plant. Mol. Biol.* **26**, 1139–1153.

Knight, A.E. and Kendrick-Jones, J. (1993) A myosin-like protein from a higher plant. *J. Mol. Biol.* **231**, 148–154.

Kuroda, K. (1990) Cytoplasmic streaming in plant cells. *Int. Rev. Cytol.* **121**, 267–307.

La Claire, J.W., II (1991) Immunolocalization of myosin in intact and wounded cells of the green alga *Ernodesmis verticillata* (Kützing) Borgesen. *Planta*, **184**, 209–217.

La Claire, J.W., II, Chen, R. and Herrin, D.L. (1995) Identification of a myosin-like protein in Chlamydomonas Rheinhardtii (Chlorophyta). *J. Phycology*, **31**, 302–306.

Lucas, W.J., Bouché-Pillon, S., Jackson, D.P., Nguyen, L., Baker, L., Ding, B. and Hake, S. (1996) Selective trafficking of KNOTTED1 homeodomain protein and its mRNA through plasmodesmata. *Science,* **270**, 1981–1982.

Matsudeira, P. and Burgess, D.R. (1978) SDS microslab linear gradient polyacryamide gel electrophoresis. *Anal. Biochem.* **83**, 386–396.

McCurdy, D.W. and Williamson, R.E. (1991) Actin and actin-associated proteins. In *The Cytoskeletal Basis of Plant Growth and Form* (Lloyd, C.W., ed.). London: Academic Press Ltd, pp. 3–14.

McLean, B.G., Zupan, J. and Zambryski, C. (1995) Tobacco mosaic virus movement protein associates with the cytoskeleton in tobacco cells. *Plant Cell*, **7**, 2101–2114.

Mermall, V., Post, P.L. and Mooseker, M.S. (1998) Unconventional myosins in cell movement, membrane traffic and signal transduction. *Science*, **279**, 527–533.

Miller, D.D., Scordilis, S.P. and Hepler, P.K. (1995) Identification and localization of three classes of myosins in pollen tubes of *Lilium longiflorum* and *Nicotiana alata. J. Cell Sci.* **108**, 2549–2653.

Mineyuki, Y. and Gunning, B.E.S. (1990) A role for preprophase bands of microtubules in maturation of new cell-walls, and a general proposal of the function of preprophase band sites in cell-division in higher plants. *J. Cell Sci.* **97**, 527–537.

Moepps, B., Conrad, S. and Schraudolf, H. (1993) PCR-dependent amplification and sequence characterization of partial DNAs encoding myosin-like proteins in *Anemia phyllitidis* (L.) Sw. & *Arabidopsis thaliana* (L.) Heynh. *Plant Mol. Biol.* **21**, 1077–1083.

Moore, P.J. and Staehelin, L.A. (1988) Immunogold localization of the cell-wall matrix polysaccharides rhamnogalacturonan-1 and xyloglucan-1 during cell expansion and cytokinesis in trifolium pratense l. – implication for secretory pathways. *Planta*, **174**, 433–445.

Mooseker, M.S. and Cheney, R.E. (1995) Unconventional myosins. *Annu. Rev. Cell Dev. Biol.* **11**, 633–675.

Northcote, D.H. (1989) Control of plant-cell wall biogenesis – an overview. *ACS Symp Series*, **399**, 1–15.

Overall, R.L., Wolffe, J. and Gunning, B.E.S. (1982) Intercellular communication in *Azolla* roots: I. Ultrastructure of plasmodesmata. *Protoplasma*, **111**, 134–150.

Plazinski, J., Elliott, J., Hurley, U.A., Burch, J., Arioli, T. and Williamson, R.E. (1997) Myosins from Angiosperms, ferns and algae. Amplification of gene fragments with versatile PCR primers and detection of protein products with a monoclonal antibody to a conserved head epitope. *Protoplasma*, **196**, 78–86.

Qiao, L., Grolig, F., Jablonsky, P.P. and Williamson, R.E. (1989) Myosin heavy chains: Detection by immunoblotting in higher plants and localization by immunofluorescence in the alga *Chara. Cell. Biol. Int. Report*, **13**, 107–117.

Radford, J.E. and White, R.G. (1998) Localization of a myosin-like protein to plasmodesmata. *Plant J.* **14**, 743–750.

Reichelt, S., Knight, A.E., Hodge. T.P., Baluska, F., Volkmann, D. and Kendrick-Jones, J. (1997) Characterization of a plant myosin. *Mol. Biol. Cell*, **7** (Suppl.), 216a.

Samuels, A.L., Giddings,J.H., Jr and Staehelin, L.A. (1995) Cytokinesis in tobacco BY-2 and root tip cells: a new model of cell plate formation in higher plants. *J. Cell Biol.* **130**, 1345–1357.

Studier, F.W. and Moffat, B.A. (1986) Use of bacteriophage T7 RNA polymerase to direct selective high level expression of cloned genes. *J. Mol. Biol.* **189**, 113–130.

Tang, X., Hepler, P.K. and Scordilis, S.P. (1989) Immunochemical and immunocytochemical identification of a myosin heavy chain polypeptide in *Nicotiana* pollen tubes. *J. Cell. Sci.* **92**, 569–574.

Titus, M.A. (1993) Myosins. *Curr. Opin. Cell Biol.* **5**, 77–81.

Turkina, M.V., Kulikova, A.L., Sokolov, O.I., Bogatyrev, V.A. and Kursanov, A.L. (1987) Actin and myosin filaments from the conducting tissues of *Heracleum sosnowskyi, Plant Physiol. Biochem.* **25,** 689–696.

Vahey, M., Titus, M., Trautwein, R. and Scordilis S. (1982) Tomato

actin and myosin: contractile proteins from higher plants. *Cell Motil.* **2,** 131–148.

Valster, A.H. and Hepler, P.K. (1997) Caffeine inhibition of cytokinesis: Effect on the phragmoplast cytoskeleton in living *Tradescantia* stamen hair cells. *Protoplasma*, **196**, 155–166.

Vitha, S., Baluska, F., Mews, M. and Volkmann, D. (1997) Immunofluorescence detection of F-actin on low melting point wax sections from plant tissues. *J. Histochem. Cytochem.* **45**, 89–95.

Waigmann, E. and Zambryski, P. (1995) Tobacco mosaic virus movement protein-mediated protein transport between trichome cells. *Plant Cell*, **7**, 2069–2079.

White, R.G., Badelt, K., Overall, R.L. and Vesk, M. (1994) Actin associated with plasmodesmata. *Protoplasma*, **180**, 169–184.

Williamson, R.E. (1993) Organelle movements. *Annu. Rev. Plant Physiol. Plant Mol. Biol.* **44**, 181–202.

Yamamoto, K., Kikuyama, M., Sutoh-Yamamoto, N., Kamitsubo, E. and Katayama, E. (1995) Myosin from alga *Chara*: Unique structure revealed by electron microscopy. *J. Mol. Biol.* **254**, 109–115.

Yokota, E., McDonald, A.R., Liu, B., Shimmen, T. and Palewitz, B.A. (1995) Localization of a 170kDa myosin heavy chain in plant cells. *Protoplasma*, **185**, 178–187.

Yokota, E. and Shimmen, T. (1994) Isolation and characterization of plant myosin from pollen tubes of lily. *Protoplasma*, **177**, 153–162.

Zambryski, P. (1995) Plasmodesmata: Plant channels for molecules on the move. *Science*, **270**, 1943–1944.